Hydrochemical Characteristics, Toxic Element Sources, and Health Risk Assessment of Surface Waters in the Amu Darya Basin of Uzbekistan, arid Central Asia

Shuie Zhan
Nanjing Institute of Geography and Limnology Chinese Academy of Sciences
Jinglu Wu (w.jinglu@niglas.ac.cn)
Nanjing Institute of Geography and Limnology, Chinese Academy of Sciences https://orcid.org/0000-0001-9589-0322
Miao Jin
Nanjing Institute of Geography and Limnology Chinese Academy of Sciences

Research Article

Keywords: Toxic elements, Source identification, Health risk assessment, Former shoreline, Amu Darya Basin

Posted Date: April 5th, 2021

DOI: https://doi.org/10.21203/rs.3.rs-324142/v1

Version of Record: A version of this preprint was published at Environmental Science and Pollution Research on August 21st, 2021. See the published version at https://doi.org/10.1007/s11356-021-15799-x.

Hydrochemical characteristics, toxic element sources, and health risk assessment of surface waters in the Amu Darya Basin of Uzbekistan, arid Central Asia

Shuie Zhan [1, 3], Jinglu Wu [1, 2, *], Miao Jin [1, 3]

[1] *State Key Laboratory of Lake Science and Environment, Nanjing Institute of Geography and Limnology, Chinese Academy of Sciences (CAS), Nanjing 210008, China*

[2] *Research Center for Ecology and Environment of Central Asia, Chinese Academy of Sciences, Urumqi 830011, China*

[3] *University of Chinese Academy of Sciences, Beijing 100049, China*

*Corresponding author: Nanjing Institute of Geography and Limnology, Chinese Academy of Sciences, Nanjing 210008, China

E-mail address: w.jinglu@niglas.ac.cn

Tel: +86-25-86882159

Fax: +86-25-57714759

Abstract: As the core of arid Central Asia, Uzbekistan is experiencing prominent water scarcity with increasingly warming climate and accelerated human impact. To determine the hydrochemical characteristics and sources of toxic elements, as well as to assess water quality and health risks in Uzbekistan, 55 surface water samples were collected from the Amu Darya Basin of Uzbekistan (ADBU) and monitored for 20 parameters. A hierarchical cluster analysis showed that river water samples from the middle reach and Amu Darya Delta (ADD) were dominantly HCO_3-Ca and SO_4-Ca·Mg type, respectively. While the water samples collected near the former shoreline of the ADD and sewage outlets were dominantly Cl-Ca·Mg and Cl-Na types, which were consistent with the distribution of sites with high concentrations of toxic elements, seriously affected by human activities. Furthermore, principal component analysis indicated that the toxic elements of Pb and Cd in surface waters of the ADBU had industrial origins; local agricultural activities were considered to have contributed much of the NO_3, Zn, Ni, Hg and Mn through pesticides and fertilizers; and Cu, Cr, As, and Co were controlled by mixed anthropogenic and natural sources. The results of water quality and health risk assessment also suggested that unsuitable drinking waters were displayed near the former shoreline of the ADD region and sewage outlets, and human health risks also occurred these areas.

Keywords: Toxic elements; Source identification; Health risk assessment; Former shoreline; Amu Darya Basin

1. Introduction

Water resources are of great significance to social development and the ecological environment (Graham et al. 2020). In arid Central Asia, water is the most critical factor driving economic and

social development (Soliev and Theesfeld 2020). However, due to rapid population growth and climate change, water resources in Central Asia have been pushed to their natural limits and entail a series of environmental and socioeconomic issues, such as water quality deterioration, soil salinization and food crises (Bobojonov and Aw-Hassan 2014; Jalilov et al. 2018). This is especially true in Uzbekistan, the most populous country in Central Asia, which receives ultra-limited water resources from its upstream neighbours by means of shared rivers and is unable to meet its living, industrial and agricultural needs (Kundzewicz and Kowalczak 2009). In recent decades, the growing population coupled with increasing land irrigation and water resource development activities in upstream regions has led to several problems in Uzbekistan, including the disappearance of some terminal lakes. The Aral Sea, once the fourth-largest inland sea in the world, has shrunk dramatically from 68,478 km^2 in 1960 to 8,321 km^2 in 2018, exerting a huge impact on the local ecological environment, especially on the Amu Darya Delta on the edge of the lake (Whish-Wilson 2002; Yang et al. 2020). As a result of the reduction in water volume, the deterioration of water quality and the emission of pollutants, the health status of the residents in the region has declined precipitously, with high infant mortality rates, growth retardation, and high morbidity rates becoming more common, which has been considered an ecological catastrophe in the 20th century (Micklin 2007; Schiermeier 2001). Water environmental issues have become increasingly prominent in the basin (Crosa et al. 2006; Papa et al. 2004; Tornqvist et al. 2011).

Hydrochemistry can reveal the climate and environment of the watershed. Through comprehensive knowledge of the chemical compositions and hydrochemical characteristics of river water, water quality is evaluated to understand its applicability for various purposes (Wu et al. 2020). In view of this, the evolutionary processes, controlling factors and solute sources of river

hydrochemistry have been extensively studied in recent years (Hua et al. 2020). Additionally, toxic elements are one of the important indicators of environmental change. Anthropogenic activities cause the accumulation of toxic elements in the aquatic environment, posing potential health risks (Li et al. 2021). A large number of studies have been carried out on concentrations, distributions, sources and assessment of toxic elements in the world's major rivers, such as the Tigris River (Varol and Sen 2012), Subarnarekha River (Giri and Singh 2014), Huai River (Wang et al. 2017), Damodar River (Pal and Maiti 2018), Tana River (Njuguna et al. 2020), and Aharchai River (Jafarzadeh et al. 2020). Hence, studies of river hydrochemistry and toxic elements are necessary; they can provide an effective basis for ensuring water safety and protecting water resources.

As the most important water resource in Uzbekistan and the Aral Sea basin, the downstream aquatic environment of Amu Darya has always been a worldwide research focus (Crosa et al. 2006; Johansson et al. 2009; Papa et al. 2004; Tornqvist et al. 2011). However, few studies have been carried out on the combination of hydrochemistry and toxic elements in this region, which causes great uncertainty for water resource management in Uzbekistan. In an effort to fill the aforementioned knowledge gaps, we conducted a preliminary study on the surface water in the Amu Darya Basin of Uzbekistan (ADBU) that aims to (1) analyse the concentrations and spatial variations of hydrochemical characteristics and toxic elements in surface water; (2) identify probable sources and influencing factors of toxic elements via multiple statistical analyses; and (3) evaluate the suitability of surface water for applications and hazard impacts on human health based on toxic elements and hydrochemical indicators.

2. Materials and methods

2.1. Study area

Uzbekistan is located in Central Asia, between 37° and 45°N and 56° and 73°E (**Fig. 1**), with a total area of 4.489×10^5 km^2 and a total population of more than 30 million. It is completely landlocked, and plain lowlands account for 80% of the whole area, most of which are located in the Kyzylkum Desert in the northwest. The climate of Uzbekistan is continental, with high seasonal variations in air temperature and rainfall. Summers are long and hot, with an average maximum temperature of 36℃, and winters are short and cold, with an average minimum temperature of -8℃. Precipitation mainly falls during winter and spring, with average values ranging from 80 ~ 200 mm year^{-1} in the desert plain areas and 600 ~ 800 mm year^{-1} in the mountainous plateau areas. Water resources of the country are mainly fed by surface runoff from the Amu Darya and Syr Darya rivers, which are attributed to the Aral Sea Basin. The main consumer of available water resources is irrigated agriculture, which accounts for up to 90% of the total water consumption in some years (Mirshadiev et al. 2018; UENP 2016).

The Amu Darya, with a total length of 2550 km, primarily originates from snow and glacial meltwater in the Pamir Mountains, which are known as “Central Asia’s Water Tower”. The Zeravshan River (ZR) flows into the middle reach of this river and finally empties into the Aral Sea through an extensive delta (Wang et al. 2016). Due to the large-scale expansion of irrigation systems and climate warming, the average discharge of the Amu Darya contributing to the Aral Sea has declined from 78 km^3 year^{-1} to 0-1 km^3 year^{-1}, leading to many ecological problems in the region (Crosa et al. 2006; Yang et al. 2020). The most important problem is the drying up of the Aral Sea and subsequently the collapse of the local ecological environment in the lake’s

surroundings, which is particularly severe in the lower Amu Darya, an area that was declared a World Disaster Zone in 1991 (Crosa et al. 2006; Papa et al. 2004).

The Amu Darya Delta (ADD) lies on the lower Amu Darya and the southern edge of the Aral Sea (**Fig. 1**). The region covers an area of 6.3×10^4 km^2 and has a population of more than 3 million people, of whom approximately 70% are engaged in crop production, animal husbandry and horticulture (Dubovyk et al. 2013; Papa et al. 2004). The delta has an extreme continental climate. The temperature ranges from 45°C to -30°C, with an average of approximately 13°C $year^{-1}$. The average precipitation is less than 100 mm $year^{-1}$, and the potential evaporation exceeds 1000 mm $year^{-1}$ (Jarsjo et al. 2017). Therefore, it relies entirely on upstream runoff flowing through rivers and canals for agricultural irrigation and livelihoods. Over the past few decades, however, the Amu Darya has dried up before reaching the former shoreline of the Aral Sea (Tornqvist et al. 2011). Low precipitation, dry climate, and high evaporation combined with human activities have led to the region becoming one of the most sensitive and ecologically fragile areas in Uzbekistan.

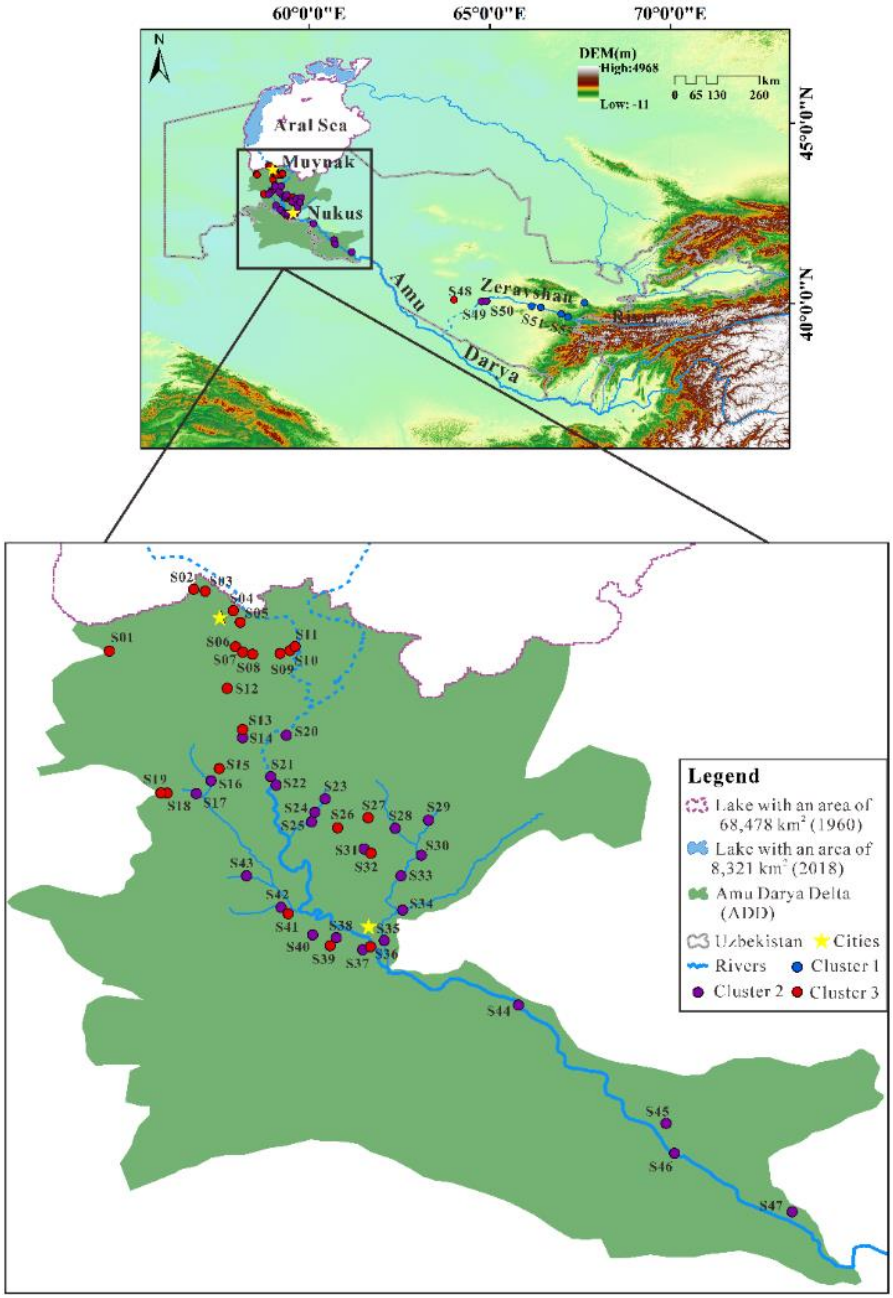

Fig 1 Geographical location of the study area and sampling sites

2.2. Sample collection and analysis

In August 2019, a field survey was conducted across the ADBU that covered its main regions, including the ADD and ZR see **Fig. 1**. A total of 55 water samples (including river water, ditch water, and drainage water) were collected at a depth of approximately 30 cm below the surface.

Among them, S10 and S48 were representative sampling sites with serious pollution in the ADD and ZR, respectively. The geographical locations of each sampling site were recorded with a portable GPS. Each water sample was filtered immediately through a 0.45 μm Millipore nitrocellulose filter (Merck-Millipore) and then subdivided into two parts: one part was stored for anion analysis, while the other was acidified with ultra-pure HNO_3 to a pH < 2 for cation and toxic element analysis. Prior to laboratory analysis, all collected water samples were refrigerated at a temperature of approximately 4°C.

The pH and total dissolved solids (TDS) were measured using a multi-parameter YSI 6500 water quality analyser (USA), and carbonate (HCO_3^-) alkalinity was measured by titration using HCl and methyl orange dye indicators. The major cations (K^+, Na^+, Ca^{2+} and Mg^{2+}) were determined by inductively coupled plasma mass spectrometry using model ICP-OES (Prodigy, USA) with detection limits of 0.1 ppm for K^+, 0.03 ppm for Na^+, 0.01 ppm for Ca^{2+}, and 0.003 ppm for Mg^{2+}. Additionally, anions (SO_4^{2-} and Cl^-) were determined by ion chromatography with an ICS-2000 (Dionex Corporation, USA). The detection limits for Cl^- and SO_4^{2-} were 0.18 and 0.05 ppm, respectively. The average analytical precision for all ions was better than 5%, and the field blanks during the measurements were very low, with most of them registering as below the detection limit.

The concentrations of toxic elements were analysed by an ICP-MS 7700x (PerkinElmer Inc., USA) under optimum analytical conditions. After the initial calibration, a standard was inserted between every 10 samples to ensure data accuracy. Based on their toxicities and potential environmental risks from the perspective of water pollution, as well as their wide application and detection in recent years, the toxic elements investigated in this study were copper (Cu), zinc (Zn),

manganese (Mn), cadmium (Cd), chromium (Cr), cobalt (Co), nickel (Ni), lead (Pb), mercury (Hg), and arsenic (As), and their detection limits were 0.01, 0.1, 0.02, 0.005, 0.05, 0.005, 0.03, 0.01, 0.02, and 0.05 ppb, respectively.

2.3. Water quality assessment

The water quality index (WQI) is the rate reflecting the combined impact of different water quality variables, and it is considered a powerful tool that can present a comprehensive picture of water quality in the study area, calculated as follows:

$$\boldsymbol{WQI = \sum[W_i \times (\frac{C_i}{S_i})] \times 100} \quad (1)$$

where W_i represents the weight of each parameter *i* and the relative importance of each individual water quality parameter used for drinking. It is calculated according to the eigenvalues of each principal component and the factor loading of each parameter in a principal component analysis (PCA) of all physicochemical parameters (Wang et al. 2017). The values of W_i are summarized in the supplementary material (**Table S1**). C_i is the measured concentration of elements or ions in water samples, and S_i is the World Health Organization concentration for each element or ion (WHO 2011). Accordingly, water quality can be divided into five different classifications: excellent water quality ($0 \leq WQI < 50$); good water quality ($50 \leq WQI < 100$); poor water quality ($100 \leq WQI < 200$); very poor water quality ($200 \leq WQI < 300$); and water unsuitable for drinking ($WQI \geq 300$).

2.4. Health risk assessment

Here, human health risks associated with a specific chemical were considered primarily

non-carcinogenic risks. For the health risk assessment of toxic elements, direct ingestion and dermal absorption are the two primary modes of toxic element exposure from water sources, so they are usually considered (Mahato et al. 2016). According to the risk guidelines of the USEPA (USEPA 2004), the exposure dose for direct ingestion ($ADD_{ingestion}$) and dermal absorption (ADD_{dermal}) were calculated as follows:

$$ADD_{ingestion} = \frac{C_w \times IR \times EF \times ED}{BW \times AT} \quad (2)$$

$$ADD_{dermal} = \frac{C_w \times SA \times K_p \times EF \times ET \times ED \times 10^{-3}}{BW \times AT} \quad (3)$$

where C_w is the concentration of toxic elements in water samples (μg/L); *IR* is the ingestion rate (L/day); *EF* is the exposure frequency (days/year); *ED* is the exposure duration (years); *BW* is the body weight (kg); *AT* is the average time for non-carcinogens (days); *SA* is the exposed skin area (cm^2); *Kp* is the dermal permeability coefficient in the samples (cm/h); and *ET* is the exposure time (h/day). The specific values of the parameters are given in **Table S2.**

The potential non-carcinogenic risks were assessed by the hazard quotient (*HQ*). The total potential non-carcinogenic risks caused by two different pathways was expressed as a hazard index (HI), which was defined as:

$$Hazard\ Quotient(HQ) = ADD/RfD \quad (4)$$

$$Hazard\ Index(HI) = \sum(HQ_{ingestion} + HQ_{dermal}) \quad (5)$$

where *RfD* is the reference dose (μg/kg/day), $RfD_{dermal} = RfD_{ingestion} \times ABS_g$, and ABS_g is the gastrointestinal absorption factor (dimensionless); see **Table S2**. $HQ_{ingestion}$ is the hazard quotient from direct ingestion and HQ_{dermal} is the hazard quotient from dermal absorption. When values of HQ are > 1, non-carcinogenic effects should be considered. Similarly, an HI < 1 indicates that the

198 measured element has a small adverse health impact on local residents, and an HI ≥ 1 indicates a
199 greater likelihood of an adverse health impact.
200
201 2.5. Statistical analysis
202 On the basis of hydrochemistry and toxic elements, water samples were classified into
203 different types controlled by natural and/or human processes using hierarchical clustering analysis
204 (HACA), which was plotted with SPSS 25.0. In addition, combined with water chemistry, the
205 sources of toxic elements in surface water were identified by PCA, which was performed by SPSS
206 25.0 and Canoco 5.0. ArcGIS 10.2 software was used to visualize the WQI and HI outcomes and
207 display their spatial distribution.
208
209 **3. Results and discussion**
210 3.1. Spatial patterns of hydrochemical characteristics in surface water
211 Surface water showed slightly alkaline characteristics with pH values of 8.12 ± 0.15 and 7.91 ±
212 0.46 in the ZR and ADD, respectively **(Table 1)**. The variation of TDS in water may be related to
213 the patterns and intensity of human activity, as well as pollution (Han and Liu 2004). The surface
214 water in the ADD had an average value of TDS=1332 mg/L, ranging from 242 to 8902 mg/L,
215 which is larger than that (283 mg/L) of large rivers worldwide (Gaillardet et al. 1999). The ZR
216 water clearly had a lower average TDS value (322 mg/L). The contaminated water, S10, showed
217 the highest value (TDS=119827 mg/L), while several ZR samples near the mountain pass, which
218 were less affected by human activity, had the lowest TDS values.
219 According to a statistical analysis of hydrochemical parameters, the abundance of cations was

220 Ca^{2+}> Na^{+} > Mg^{2+}> K^{+} in the ZR. The concentrations of Ca^{2+} and Na^{+} ranged from 34.91 to 104
221 mg/L and 2.26 to 92.10 mg/L, with average values of 55.86 mg/L and 28.01 mg/L, respectively.
222 The mean concentrations of Mg^{2+} and K^{+} were 14.74 mg/L and 2.98 mg/L, respectively **(Table 1)**.
223 For the ADD water, the abundance of cations was Na^{+} > Ca^{2+} > Mg^{2+}> K^{+}. Na^{+} and Ca^{2+} ranged
224 from 32.93 to 1894 mg/L and 51.50 to 664 mg/L, with average values of 261 mg/L and 145 mg/L,
225 respectively. The mean concentrations of Mg^{2+} and K^{+} were 77 mg/L and 9.55 mg/L, respectively
226 **(Table 1)**. Na^{+} and Ca^{2+} were the predominant cations in the ADBU.

227 Anion concentrations were on the order of HCO_3^{-}> SO_4^{2-}> Cl^{-} in the ZR water. The HCO_3^{-}
228 concentration ranged from 135.6 to 228.8 mg/L with an average value of 182.2 mg/L. The
229 observed concentrations of SO_4^{2-} and Cl^{-} ranged from 37.18 to 325.9 mg/L and 1.02 to 77.3 mg/L,
230 with mean values of 115.1 mg/L and 22.99 mg/L, respectively **(Table 1)**. For the ADD water, the
231 abundance of anions was SO_4^{2-}> Cl^{-}> HCO_3^{-}. The concentrations of SO_4^{2-} and Cl^{-} ranged from
232 77.62 to 3036 mg/L and 1.77 to 2760 mg/L, with average values of 386 mg/L and 233 mg/L,
233 respectively. The concentrations of HCO_3^{-} ranged from 67.05 to 390 mg/L with an average value
234 of 160 mg/L **(Table 1)**. HCO_3^{-} was the predominant anion in the ZR, while the water in the ADD
235 was dominated by SO_4^{2-} and Cl^{-}. In general, compared with the world average, the ion
236 concentrations in the surface water of the ADD were at a high level (Gaillardet et al. 1999).

237

238 **Table 1** Statistical analysis of hydrochemical parameters and toxic elements concentrations in surface water samples across the ADBU

Parameters	ADD					ZR					WHO Standards	World average
	Min	Max	Ave	SD	S10	Min	Max	Ave	SD	S48		
pH	6.64	8.55	7.91	0.46	7.44	7.96	8.35	8.12	0.15	7.95	6.5-8.5[a]	---
TDS(mg/L)	242	8902	1332	1771	119827	94	865	322	256	2358	1000[a]	283[c]
Ca^{2+}(mg/L)	51.50	664	145	121	478	34.91	104	55.86	28.1	298	200[a]	30.26[c]
K^{+}(mg/L)	2.88	47	9.55	8.96	1440	2.04	4.34	2.98	0.85	23.88	---	3.48[c]
Mg^{2+}(mg/L)	10.59	467	77	102	14303	4.92	31.9	14.74	9.98	250	150[a]	34.64[c]
Na^{+}(mg/L)	32.93	1894	261	369	56949	2.26	92.10	28.01	35.83	433	200[a]	11.41[c]
Cl^{-}(mg/L)	1.77	2760	233	510	71314	1.02	77.3	22.99	31.28	894	250[a]	48.60[c]
SO_4^{2-}(mg/L)	77.62	3036	386	580	54268	37.18	325.9	115.1	113.5	900	250[a]	37.58[c]
HCO_3^{-}(mg/L)	67.05	390	160	75.1	872	135.6	228.8	182.2	31.50	199	250[a]	110.61[c]

NO_3-N (mg/L)	0.02	59.43	1.45	8.64	0.58	0.02	1.19	0.62	0.36	2.43	11.0[a]	---
Cu(μg/L)	0.61	2.85	1.31	0.47	29.82	0.169	1.25	0.51	0.44	1.13	2000[a]	1.48[d]
Zn(μg/L)	9.60	82.87	22.6	12.41	21.16	14.08	34.61	24.14	7.50	17.98	5000[b]	0.60[d]
Mn(μg/L)	0.42	839	49	155	335	0.693	6.69	3.17	2.59	5.64	400[a]	34.0[d]
Cd(μg/L)	n.a	1.50	0.05	0.22	0.17	0.005	0.05	0.02	0.02	0.01	3[a]	0.080[d]
Cr(μg/L)	0.75	1.41	0.94	0.13	5.54	0.865	1.60	1.201	0.26	0.92	50[a]	0.70[d]
Co(μg/L)	0.03	3.32	0.28	0.53	5.72	0.044	0.11	0.07	0.03	0.32	50[a]	0.148[d]
Ni(μg/L)	0.25	11.81	0.91	1.68	4.31	0.364	0.61	0.45	0.09	1.08	70[a]	0.80[d]
Pb(μg/L)	0.12	2.25	0.25	0.31	1.48	0.120	0.23	0.172	0.04	0.20	10[a]	0.079[d]
Hg(μg/L)	n.a	0.19	0.03	0.03	n.a	n.a	0.024	0.012	0.005	n.a	6[a]	---
As(μg/L)	0.75	14.00	3.81	2.50	87.18	0.624	1.80	1.29	0.42	3.33	10[a]	0.62[d]

239 [a] WHO drinking water guidelines (WHO 2011); [b] USEPA drinking water standards (USEPA 2010); [c] Gaillardet et al. (1999); [d] Gaillardet, et al. (2005).

240

241 3.2. Hydrochemical facies of surface water

242 The Chadha diagram was used to classify major hydrochemical types in the ADBU, and it
243 can help in understanding the role of major ions (both cations and anions) in water chemistry
244 (Chadha 1999). This classification is based on the relationship between differences in alkaline
245 earths (Ca^{2+} + Mg^{2+}) and alkali metals (Na^{+} + K^{+}) and weak acidic anions (CO_3^{2-} + HCO_3^{-})
246 and strong acidic anions (Cl^{-} + SO_4^{2-}). Four fields within the diagram containing four different
247 types of hydrochemical facies were obtained **(Fig. 2)**. In the study area, 49.1% (n=27) of the
248 water samples were SO_4-Ca·Mg type, which was dominated by Ca^{2+} and SO_4^{2-}, potentially
249 representing the influence of water-rock interactions. Two of these samples were collected
250 from the ZR, and the others were collected from the ADD **(Fig. 2)**. Of the remaining samples,
251 9% (n=5) were HCO_3-Ca type, which was formed by the reactions of CO_{2-} and $CaCO_3$-bearing
252 minerals in the recharge zones of rainwater areas (Raj and Shaji 2017), and these samples
253 were all from the ZR. Out of all the water samples, 34.5% (n=19) were in the Cl-Ca·Mg type
254 category, and 7% (n=4) were in the Cl-Na type category; the high Cl^{-} abundances indicated
255 strong effects of evaporation processes or human activities, which led to an increase in the
256 concentration of Cl^{-} (Gaillardet et al. 1999). All of these samples were from the ADD, with the
257 exception of one from the ZR. The hydro-facies distribution showed that the trend in the water
258 type of the basin followed the order HCO_3-Ca < (Cl-Ca·Mg + Cl-Na) < SO_4-Ca·Mg,
259 indicating serious effects by human activities and arid climate.

260

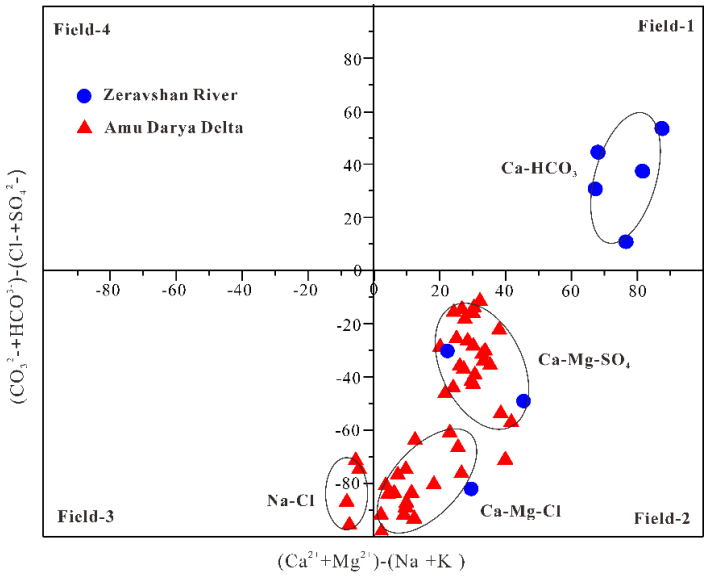

Fig 2 Chadha diagram demonstrating the hydrochemical classification of surface waters in the ADBU

3.3. Mechanisms controlling the hydrochemistry

The hydrochemical compositions and characteristics are generally controlled by inputs through natural processes (Gao et al. 2020; Gibbs 1970) and human activities (An et al. 2020; Gaillardet et al. 1999). The natural mechanisms controlling the hydrochemistry of surface water can be inferred from the three end members in the Gibbs schematic diagram (**Fig. 3**). Based on the ratio of Na/(Na+ Ca) and Cl/(Cl + HCO_3) with respect to TDS in water, Gibbs divided the plot into three domains: rock dominance, evaporation dominance and precipitation dominance (Gibbs 1970). As shown in **Fig. 3**, all but one of the water samples in the evaporation dominance zone were from the ADD, which was characterized by high ratios of Na/(Na + Ca) and Cl/(Cl + HCO_3) and high concentrations of TDS, suggesting that evaporative crystallization was the primary source controlling the water chemistry. Five water samples from the ZR were in the rock dominance zone, which were characterized by low ratios of Na/(Na + Ca) and Cl/(Cl + HCO_3) and moderate concentrations of TDS, indicating the influence of rock weathering. The other samples were in an intermediate state, with moderate TDS and Na/(Na + Ca) and Cl/(Cl + HCO_3) ratios, which were controlled by both rock weathering and evaporative crystallization processes. In addition, in some heavily polluted rivers, the major element chemistry was dominated by human activities, such as in the Elbe and Wisla Rivers, which are dominated by wastewater discharges from coal and salt mines (Gaillardet et al. 1999).

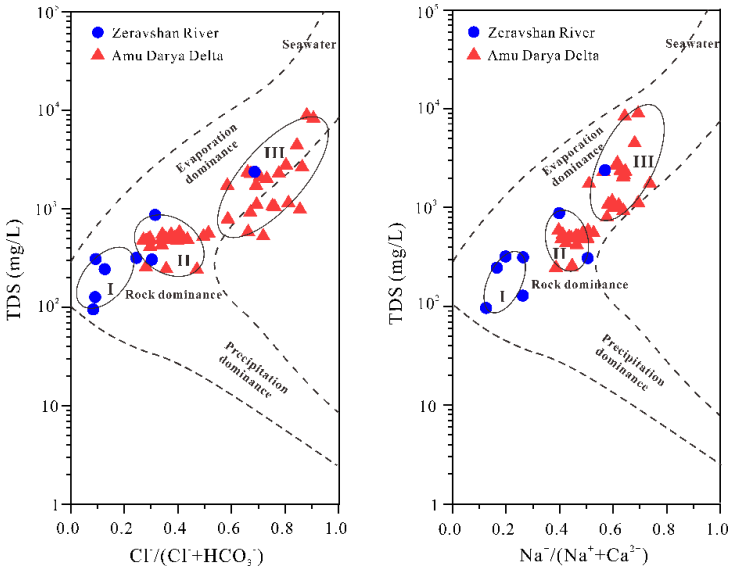

Fig 3 Gibbs diagram showing the main natural processes controlling hydrochemistry

3.4. Spatial variability of toxic element concentrations

Spatial heterogeneity of anthropogenic activities (industrial, agricultural, and domestic) and the natural elemental background in different districts of the basin led to different distributions of toxic elements. Overall, the variation in toxic element concentrations in surface waters of the ADBU was significant, especially in Mn and Zn, which had larger SD values than other elements **(Table 1)**. According to their mean values, toxic elements were divided into three categories: elements with high abundance (> 20 μg/L), elements with moderate abundance (1 to 20 μg/L), and elements with low abundance (<1 μg/L); these three categories contained Mn and Zn; As and Cu; and Cr, Cd, Co, Ni, Pb and Hg, respectively. With the exception of Zn and Cr, the mean concentrations of toxic elements in surface waters of the ADD were higher than those of the ZR **(Table 1)**. Similarly, the concentrations of toxic elements in most water samples of the ADD were also higher than those in the ZR (see **Fig. 4**). Among them, S10 had the highest concentrations of Cu, Cr, Co and As; S02 had the highest concentrations of Zn, Ni and Hg; S03 had the highest concentration of Mn; and S12 had the highest concentrations of Cd and Pb. Moreover, the concentrations of Mn and As in some samples exceed the WHO guidelines, indicating that the water in the ADD was relatively seriously polluted by toxic elements.

Compared with other rivers in the world, the toxic elements in the surface water of the ADBU

were at moderate levels. The concentrations of Cu, Zn, and Cr in the water were higher than those in the Tana River (Njuguna et al. 2020) and Aharchai River (Jafarzadeh et al. 2020). However, compared with some famous seriously polluted rivers, such as the Tigris River (Varol and Sen 2012), Huai River (Wang et al. 2017), and Damodar River (Pal and Maiti 2018), the ADBU had lower concentrations of toxic elements.

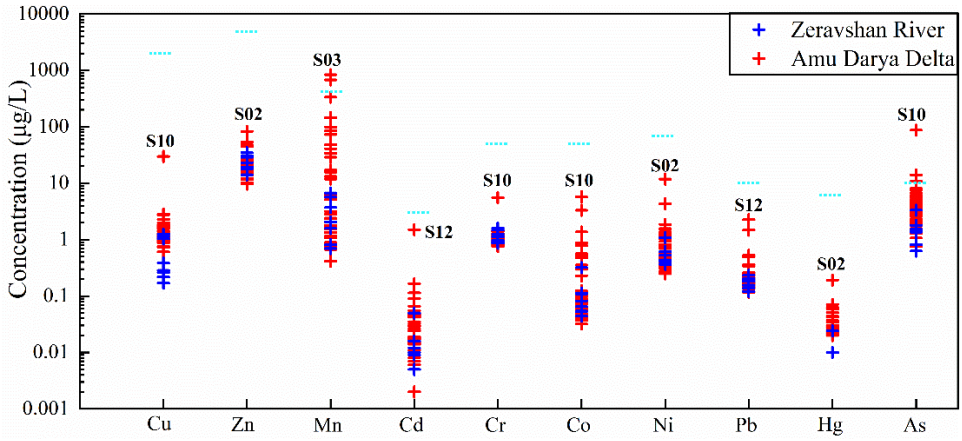

Fig 4 The toxic element concentrations of surface water in the ADBU. The blue dotted line indicates the drinking water standards of the WHO (2011)

3.5. Sample classification

A hierarchical cluster analysis (HACA) indicated groupings of samples by linking inter-sample similarities and illustrated the overall similarity of variables in the dataset (Vega et al. 1998). The cluster classifications varied with significance level because the sampling sites in these clusters had similar features and natural/anthropogenic background source types. Based on physical and chemical parameters, hierarchical agglomerative clustering by the average linkage method (between groups) was used for sample classification, rendering a dendrogram with three statistically significant clusters at (Dlink/Dmax) × 100 < 15. Cluster 1, cluster 2, and cluster 3 contained 5 (S51-S55), 27 (S14, S16-S17, S20-S25, S28-S31, S33-S35, S37-S38, S40, S42-S47, and S49-S50) and 23 (S01-S13, S15, S18-S19, S26-S27, S32, S36, S39, S41, and S48) water sampling sites, respectively (**Fig. 5**).

The distribution of sampling sites in each group is shown in **Fig. 1**. Spatially, the samples in

cluster 1 were all collected near the mountain pass in the ZR, while the samples in cluster 2 were distributed in two regions. These two groups basically belonged to river water samples, with relatively low concentrations of toxic elements and TDS, that were primarily affected by natural processes. Cluster 1 was mainly controlled by rock weathering, while cluster 2 was controlled by both rock weathering and evaporative crystallization processes, corresponding to HCO3-Ca type and SO_4-Ca·Mg type, respectively. Cluster 3 was mostly collected from sewage outlets and near the former shoreline of the ADD region. In addition to being controlled by strong natural evaporation processes, it was also affected by human activities. The samples in this group had relatively high abundances of Cl^-, toxic elements and TDS, and the hydrochemical types were mainly Cl-Ca·Mg and Cl-Na types. Under the complex influence of strong evaporation and anthropogenic activities, the hydrochemical characteristics of this group changed significantly compared with those of the other two groups.

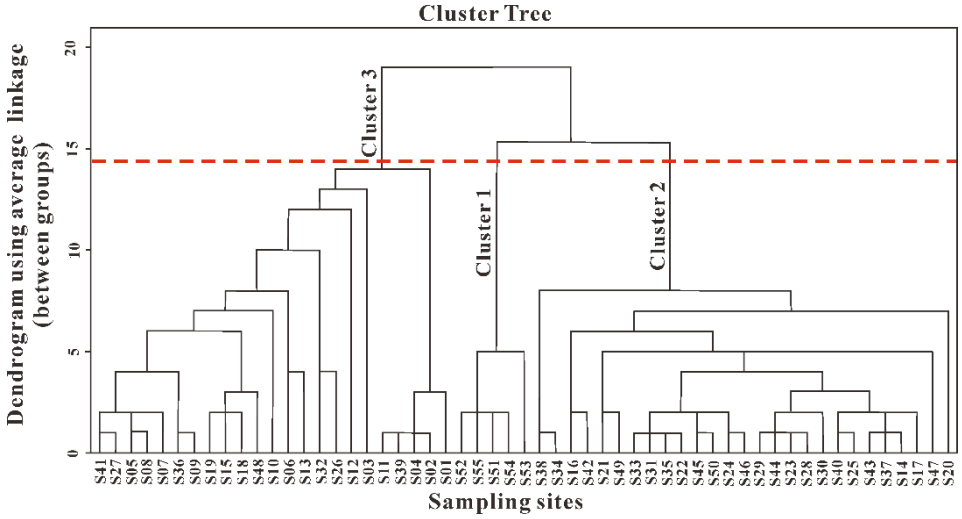

Fig 5 Dendrogram based on agglomerative hierarchical clustering for water samples in the ADBU.

3.6. Source identification of toxic elements

To analyse the sources of toxic elements in surface waters of the ADBU, SPSS and Canoco software were used to carry out PCA. The Kaiser-Meyer-Olkin (KMO) scores (0.823) and Bartlett's sphericity test values (p=0.000) indicated that the datasets were appropriate for PCA (Wang et al. 2017). As shown in **Fig. 6b**, by Canoco software, PCA extracted a total of two

dimensions that explained 89.10% of the variation in the distribution of chemical compositions. Two dimensions divided the 55 sampling sites into four quadrants. Cluster 1 and cluster 2 were mainly distributed in the second and third quadrants, which represented inputs from natural sources with weak human influence. Cluster 3 was mainly distributed in the first and fourth quadrants, which probably represented inputs from anthropogenic sources.

By SPSS, three principal components elucidated 86.0% of the variance in the analysed dataset and were all distributed in the sampling sites of cluster 3 (**Fig. 6**). TDS, Na^+, Mg^{2+}, K^+, SO_4^{2-}, Cl^-, HCO_3^-, Cu, Cr, As, and Co had high positive loadings in PC1, which elucidated 55.57% of the variances in the data matrix (**Fig. 6a**). As mentioned above, high concentrations of Cl^- and TDS may indicate that surface water was subject to intense evaporation or human activities. The arid climate resulted in the strong evaporation and concentration of water in this area (Jarsjo et al. 2017). Cu, Cr, As, and Co in water are mainly ascribed to anthropogenic sources through domestic sewage and agrochemical and industrial wastes (Habib et al. 2020; Islam et al. 2020; Wang et al. 2017). Hence, the association of TDS, Na^+, Mg^{2+}, K^+, SO_4^{2-}, Cl^-, Cu, Cr, As, and Co reflected the comprehensive influence of natural processes and various human activities on water pollution. Spatially, PC1 mainly included S36, S15, S04, S05, S07, S48, S18, S19 and S10, which were located near urban sewage outlets or the former shoreline of the ADD region (**Fig. 6b**). Untreated municipal sewage and industrial and agricultural wastewater were the main pollution sources of these water samples, such as S48 and S10.

PC2 explained 21.03% of the variance, with strong positive loadings of NO_3, Zn, Ni, and Hg and moderate loadings of Ca (0.66) and Mn (0.70) (**Fig. 6a**). It mostly included the S01-S03, S08, S11, S26-S27, S32, S39 and S41 sampling sites, which were located in the drainage outlets of the irrigated farming area or near the former shoreline of the ADD region (**Fig. 6b**). The high contents of NO_3, Zn, Ni, Hg and Mn in the water samples may be related to the extensive agricultural activities in this area (Chanpiwat and Sthiannopkao 2014). To increase crop yield, a large number of nitrogen fertilizers and pesticides have been used in the ADD, resulting in the spread of toxic chemicals in farmland (Glantz 1999). In addition, NO_3 formed by nitrogen fertilizers was susceptible to loss through leaching, which contributed to surface water and groundwater pollution in the area (Egamberdiyeva et al. 2001).

Cd and Pb exhibited high loadings in PC3, explaining 8.41% of the variance, which only occurred in S12, indicating that it may be a point source pollution (**Fig. 6**). Cd and Pb mainly originate from industries near the sampling point, including the textile industry, leaded gasoline industry and chemical manufacturing industry (Islam et al. 2020; Islam et al. 2015; Kumar et al. 2017; Zeng et al. 2015).

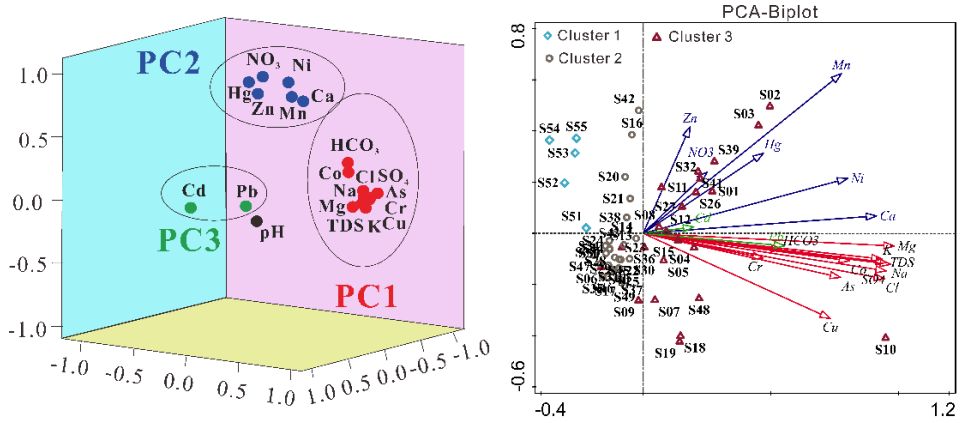

(a) (b)

Fig 6 Principal component analysis (PCA) for toxic elements in surface waters in the ADBU. (a) Component plot in rotated space by using SPSS, and (b) loading plot in two dimensions by using Canoco.

3.7. Water quality and health risk assessment

3.7.1 Suitability for drinking purposes

Given that surface water represents a major water resource for regional inhabitants, the WQI was applied to obtain a more comprehensive understanding of surface water quality for drinking purposes in the ADBU. The calculated WQI values of water ranged from 7.87 to 195.85, with an average value of 35.91, except for sample S10 (with a value of 6706.7). As shown in **Fig. 7**, of 55 water samples, there were two samples with undrinkable water quality, two samples with very poor water quality and two samples with poor water quality, which were located near the former shoreline of the ADD region and sewage outfalls. Water at other sites of the ADBU plotted in the good water or excellent water categories, with WQI values less than 100, indicating that the water was suitable for drinking. Overall, the surface water in the ADBU was in good condition; only 12.6% of water samples were unsuitable for drinking, 23.4% of samples had good quality, and

63.8% of samples had excellent quality. However, more attention should be paid to the sites near the former shoreline of the ADD region and sewage outfalls, where water would require salinity and pollutant control to reduce the drinking hazard.

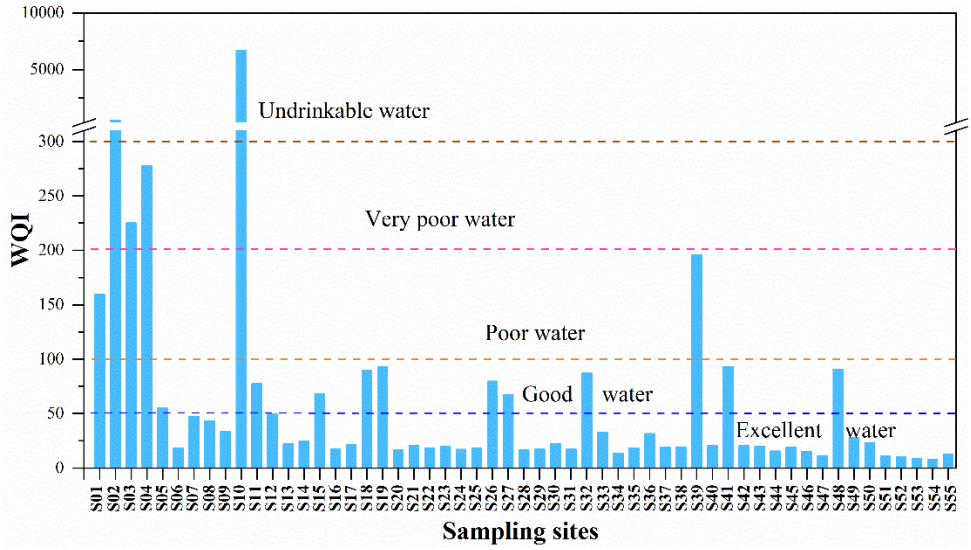

Fig 7 Water quality assessment by WQI values of surface water in the ADBU.

3.7.2 Human health risk assessment

Based on traditional risk assessment guidance (USEPA 2004), the risk of non-carcinogens to individual health of the toxic elements in surface waters from the ADBU were estimated. **Table S3** presents the HQ and HI for the direct ingestion and dermal pathways relating to adults and children in the ZR and ADD regions, respectively.

In the ADD region, $HQ_{ingestion}$ values of all elements, except As and Mn, were less than 1, suggesting that these elements posed little hazard. However, the maximum $HQ_{ingestion}$ values for As (8.56 for adults and 8.92 for children) were more than 1, and the Mn values (1.03 for adults and 1.07 for children) were near 1, which implied that As and Mn may cause adverse health effects and potential non-carcinogenic concerns. The HQ_{dermal} of all the elements for adults and children were below 1, indicating that these elements posed little hazard via dermal absorption. The decreasing order of the average HI values was As > Mn > Co > Cr > Pb > Cd > Hg > Zn > Ni > Cu, indicating that the highest contributor to chronic risks was As, followed by Mn, while the lowest were Ni and Cu for both adults and children.

In the ZR region, the $HQ_{ingestion}$ and HQ_{dermal} for both age populations of all the elements were below 1, the highest being for As, followed by Cr. In addition, in our study, the levels of the $HQ_{ingestion}$ and HQ_{dermal} were larger in children than in adults, indicating that children are more vulnerable and more exposed to health hazard effects of toxic element exposure from water, which was similar to previous findings (Habib et al. 2020; Njuguna et al. 2020).

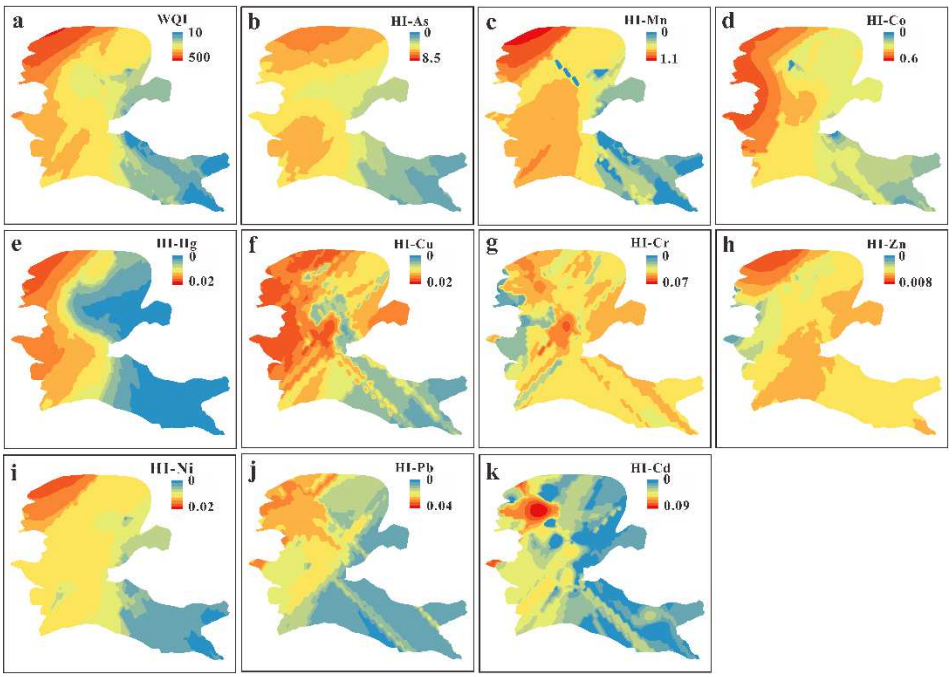

Fig 8 Spatial variations in the WQI (a) and HI (b-k) values for surface water in the ADD.

The spatial variations in water quality and health risk assessment results (the HI values for adults) in the ADD are shown in **Fig. 8**. The highest values of WQI and HI occurred near the former shoreline, indicating that the shoreline zone is the area with the most serious toxic elemental pollution and the worst water quality within the whole ADBU. Among them, the HI values of As, Mn, Co, Hg, Cu, Cr and Zn were basically consistent with the WQI results. The areas with the highest values were concentrated near the former shoreline, followed by the outfalls near the city of Nukus **(Fig. 8a ~ h)**. Additionally, the highest HI values of Cd, Pb and Ni primarily appeared near the former shoreline **(Fig. 8i ~ k)**. Due to the geographical location of the delta far downstream in the basin, the waters from irrigated lands and industrial wastewater have large amounts of salts, pesticides and toxic elements (Crosa et al. 2006; Papa et al. 2004). In addition, the displacement of the shoreline results in a drop in the groundwater level, which blocks

437 the exchange of surface water and groundwater, intensifies evaporation, and causes further
438 deterioration of water quality in the flat areas of the ADD (Shibuo et al. 2006; Vitola et al. 2012).
439 Generally, the complex combination of geographical location, hydrological conditions and
440 climatic conditions makes the shoreline the most seriously polluted water in the whole basin.
441
442 **4. Conclusions**
443 Uzbekistan, especially the ADD region near the Aral Sea, has suffered from water volume loss
444 and water quality degradation, which induces serious ecological disasters. In this study, we
445 investigated the hydrochemistry and distribution of toxic elements, further analysed the
446 endogenous factors affecting the sources of toxic elements combined with hydrochemistry, and
447 evaluated the water quality and health status of the surface water in the ADBU. The results
448 indicated that the hydrochemistry of surface water in the ADD was slightly alkaline, and the
449 average value of TDS was 1332 mg/L, which was much higher than that of the ZR (322 mg/L)
450 and the world's large rivers. Similarly, compared with the ZR region, the average
451 concentrations of toxic elements in the surface water of the ADD region were relatively high, and
452 As and Mn in some waters exceeded WHO guidelines. In the whole ADBU, there were four
453 main hydrochemical types, ordered HCO_3-Ca < (Cl-Ca·Mg + Cl-Na) < SO_4-Ca·Mg. Among
454 them, the Ca-HCO_3 type was dominant near the mountain pass in the ZR, controlled by rock
455 weathering. The hydrochemical type of other river water samples in the ADBU was primarily
456 Ca-Mg-SO_4, which was controlled by rock weathering and evaporative crystallization. The
457 surface waters near the former shoreline of the ADD region and sewage outfalls were
458 dominated by Cl-Ca·Mg and Cl-Na, which were seriously affected by human activities. PCA
459 identified three important factors that accounted for 86.0% of the total variance, indicating
460 that anthropogenic activities of industrial wastes contributed to Pb and Cd; NO_3, Zn, Ni, Hg
461 and Mn were closely related to local agricultural activities, whereas Cu, Cr, As, and Co were
462 controlled by mixed anthropogenic and natural sources. According to the WQI and HQ/HI
463 results, the worst water quality and the highest degree of potential human health risk were
464 found near the former shoreline of the ADD region. These assessments highlight the adverse
465 effects that the complex combination of geographical location, hydrological conditions and

466 climatic conditions has on the aquatic environment near the former shoreline of the ADD
467 region compared with other areas. The results also revealed that As had the greatest impact on
468 the health of local residents in the ADBU; therefore, controlling and remediating this element
469 is of utmost importance.
470
471 **Declarations**
472 **Ethical Approval and Consent to Participate**
473 Not applicable
474 **Consent to Publish**
475 Not applicable
476 **Availability of data and materials**
477 The data sets supporting the results of this article are included within the article.
478 **Competing Interests**
479 The authors declare that they have no competing interests.
480 **Funding**
481 The study was supported by the National Natural Science Foundation of China (41671200, and
482 U1603242), the Strategic Priority Research Program of Chinese Academy of Sciences, Pan-Third
483 Pole Environment Study for a Green Silk Road (XDA2006030101).
484 **Authors Contributions**
485 Shuie Zhan: Conceptualization, Software, Data curation, Writing- original draft.
486 Jinglu Wu: Funding acquisition, Investigation, Writing - review & editing, Validation.
487 Miao Jin: Investigation.
488 **Acknowledgments**
489 We thank the CAS Research Center for Ecology and Environment of Central Asia for assistance
490 with this work, Huawu Wu and Beibei Shen for field and experimental assistances.
491
492
493
494

495 **References**

496 An SK, Jiang CL, Zhang WX, Chen X (2020) Influencing factors of the hydrochemical
497 characteristics of surface water and shallow groundwater in the subsidence area of the Huainan
498 Coalfield. Arab J Geosci 13, 191. https://doi.org/10.1007/s12517-020-5140-3

499 Bobojonov I, Aw-Hassan A (2014) Impacts of climate change on farm income security in Central
500 Asia: An integrated modeling approach. Agric Ecosyst Environ 188, 245-255.
501 https://dx.doi.org/10.1016/j.agee.2014.02.033

502 Chadha DK (1999) A proposed new diagram for geochemical classification of natural waters and
503 interpretation of chemical data. Hydrogeol J 7, 431-439. https://doi.org/10.1007/s100400050216

504 Chanpiwat P, Sthiannopkao S (2014) Status of metal levels and their potential sources of
505 contamination in Southeast Asian rivers. Environ Sci Pollut R 21, 220-233.
506 https://doi.org/10.1007/s11356-013-1858-8

507 Crosa G, Stefani F, Bianchi C, Fumagalli A (2006) Water security in Uzbekistan: Implication of
508 return waters on the Amu Darya water quality. Environ Sci Pollut R 13, 37-42.
509 https://doi.org/10.1065/espr2006.01.007

510 Dubovyk O, Menz G, Conrad C, Kan E, Machwitz M, Khamzina A (2013) Spatio-temporal
511 analyses of cropland degradation in the irrigated lowlands of Uzbekistan using remote-sensing
512 and logistic regression modeling. Environ Monit Assess 185, 4775-4790.
513 https://doi.org/10.1007/s10661-012-2904-6

514 Egamberdiyeva D, Mamiev M, Poberejskaya SK (2001) The influence of mineral fertilizer
515 combined with a nitrification inhibitor on microbial populations and activities in calcareous
516 Uzbekistanian soil under cotton cultivation. Sci World J 1(S2), 108-13.
517 https://doi.org/10.1100/tsw.2001.301

518 Gaillardet J, Dupre B, Louvat P, Allegre CJ (1999) Global silicate weathering and CO_2
519 consumption rates deduced from the chemistry of large rivers. Chem Geol 159, 3-30.
520 https://doi.org/10.1016/S0009-2541(99)00031-5

521 Gaillardet J, Viers J, Dupré B (2005) Trace elements in river waters. Surface and Ground Water,
522 Weathering, and Soils 5, 225-272. https://doi.org/10.1016/B0-08-043751-6/05165-3

523 Gao YY, Qian H, Ren WH, Wang HK, Liu FX, Yang FX (2020) Hydrogeochemical

524 characterization and quality assessment of groundwater based on integrated-weight water
525 quality index in a concentrated urban area. J Clean Prod 260.
526 https://doi.org/10.1016/j.jclepro.2020.121006
527 Gibbs RJ (1970) Mechanisms Controlling World Water Chemistry. Science 170, 1088-1090.
528 https://doi.org/10.1126/science.170.3962.1088
529 Giri S, Singh AK (2014) Risk assessment, statistical source identification and seasonal fluctuation
530 of dissolved metals in the Subarnarekha River, India. J Hazard Mater 265, 305-314.
531 https://doi.org/10.1016/j.jhazmat.2013.09.067
532 Glantz MH (1999) Creeping Environmental Problems and Sustainable Development in the Aral
533 Sea Basin. Cambridge University Press. https://doi.org/10.1017/CBO9780511535970
534 Graham NT, Hejazi MI, Kim SH, Davies EGR, Edmonds JA, Miralles-Wilhelm F (2020) Future
535 changes in the trading of virtual water. Nat Commun 11, 3632.
536 https://doi.org/10.1038/s41467-020-17400-4
537 Habib MA, Islam AMT, Bodrud-Doza M, Mukta FA, Khan R, Siddique MA, Phoungthong K,
538 Techato K (2020) Simultaneous appraisals of pathway and probable health risk associated with
539 trace metals contamination in groundwater from Barapukuria coal basin, Bangladesh.
540 Chemosphere 242, 125183. https://doi.org/10.1016/j.chemosphere.2019.125183
541 Han GL, Liu CQ (2004) Water geochemistry controlled by carbonate dissolution: a study of the
542 river waters draining karst-dominated terrain, Guizhou Province, China Chem Geol 204, 1-21.
543 https://doi.org/10.1016/j.chemgeo.2003.09.009
544 Hua K, Xiao J, Li SJ, Li Z (2020) Analysis of hydrochemical characteristics and their controlling
545 factors in the Fen River of China. Sustain Cities Soc 52, 101827.
546 https://doi.org/10.1016/j.scs.2019.101827
547 Li J, Chen YZ, Lu HW, Zhai WY (2021) Spatial distribution of heavy metal contamination and
548 uncertainty-based human health risk in the aquatic environment using multivariate statistical
549 method. Environ Sci Pollut R. https://doi.org/10.1007/s11356-020-12212-x
550 Islam AMT, Islam HMT, Mia MU, Khan R, Habib MA, Bodrud-Doza M, Siddique MA, Chu RH
551 (2020) Co-distribution, possible origins, status and potential health risk of trace elements in
552 surface water sources from six major river basins, Bangladesh. Chemosphere 249, 126180.

https://doi.org/10.1016/j.chemosphere.2020.126180

Islam MS, Ahmed MK, Raknuzzaman M, Habibullah-Al-Mamun M, Islam MK (2015) Heavy metal pollution in surface water and sediment: A preliminary assessment of an urban river in a developing country. Ecol Indic 48, 282-291. http://dx.doi.org/10.1016/j.ecolind.2014.08.016

Jafarzadeh S, Fard RF, Ghorbani E, Saghafipour A, Moradi-Asl E, Ghafuri Y (2020) Potential risk assessment of heavy metals in the Aharchai River in northwestern Iran. Phys Chem Earth (2002). 115, 102812. https://doi.org/10.1016/j.pce.2019.102812

Jalilov SM, Amer SA, Ward FA (2018) Managing the water-energy-food nexus: Opportunities in Central Asia. J Hydrol 557, 407-425. https://doi.org/10.1016/j.jhydrol.2017.12.040

Johansson O, Aimbetov I, Jarsjo J (2009) Variation of groundwater salinity in the partially irrigated Amudarya River delta, Uzbekistan. J Mar Syst 76, 287-295. https://doi.org/doi:10.1016/j.jmarsys.2008.03.017

Kumar M, Ramanathan AL, Tripathi R, Farswan S, Kumar D, Bhattacharya P (2017) A study of trace element contamination using multivariate statistical techniques and health risk assessment in groundwater of Chhaprola Industrial Area, Gautam Buddha Nagar, Uttar Pradesh, India. Chemosphere 166, 135-145. https://doi.org/10.1016/j.chemosphere.2016.09.086

Kundzewicz ZW, Kowalczak P (2009) The potential for water conflict is on the increase. Nature 459, 31-31. https://doi.org/10.1038/459031a

Mahato MK, Singh PK, Tiwari AK, Singh AK (2016) Risk Assessment Due to Intake of Metals in Groundwater of East Bokaro Coalfield, Jharkhand, India Expos Health 8, 265-275. https://doi.org/10.1007/s12403-016-0201-2

Micklin P (2007) The Aral Sea disaster. In: Raymond Jeanloz (eds) Annual review of earth and planetary sciences, Annual Reviews, Palo Alto 35, 47-72. https://doi.org/10.1146/annurev.earth.35.031306.140120

Mirshadiev M, Fleskens L, van Dam J, Pulatov A (2018) Scoping of promising land management and water use practices in the dry areas of Uzbekistan. Agric Water Manag 207, 15-25. https://doi.org/10.1016/j.agwat.2018.05.015

Njuguna SM, Onyango JA, Githaiga KB, Gituru RW, Yan X (2020) Application of multivariate statistical analysis and water quality index in health risk assessment by domestic use of river

582 water. Case study of Tana River in Kenya. Process Saf Environ Prot 133, 149-158.
583 https://doi.org/10.1016/j.psep.2019.11.006
584 Pal D, Maiti SK (2018) Heavy metal speciation, leaching and toxicity status of a tropical rain-fed
585 river Damodar, India. Environ Geochem Health 40, 2303-2324.
586 https://doi.org/10.1007/s10653-018-0097-9
587 Papa E, Castiglioni S, Gramatica P, Nikolayenko V, Kayumov O, Calamari D (2004) Screening the
588 leaching tendency of pesticides applied in the Amu Darya Basin (Uzbekistan). Water Res 38,
589 3485-3494. https://doi.org/doi:10.1016/j.watres.2004.04.053
590 Raj D, Shaji E (2017) Fluoride contamination in groundwater resources of Alleppey, southern
591 India. Geosci Front 8, 117-124. https://doi.org/10.1016/j.gsf.2016.01.002
592 Schiermeier Q (2001) Ecologists plot to turn the tide for shrinking lake. Nature 412, 756-756.
593 https://doi.org/10.1038/35090704
594 Shibuo Y, Jarsjo J, Destouni G (2006) Bathymetry-topography effects on saltwater-fresh
595 groundwater interactions around the shrinking Aral Sea. Water Resour Res 42, W11410.
596 https://doi.org/10.1029/2005WR004207,
597 Soliev I, Theesfeld I (2020) Benefit Sharing for Solving Transboundary Commons Dilemma in
598 Central Asia. Int J Commons 14, 61-77. https://doi.org/10.5334/ijc.955
599 Tornqvist R, Jarsjo J, Karimov B (2011) Health risks from large-scale water pollution: Trends in
600 Central Asia. Environ Int. 37, 435-442. https://doi.org/10.1016/j.envint.2010.11.006
601 UENP (2016) Third National Communication under the UN Framework Convention on Climate
602 Change. https://unfccc.int/sites/default/files/resource/TNC of Uzbekistan under.
603 USEPA (2004) Risk Assessment Guidance for Superfund Volume 1. Human Health Evaluation
604 Manual (Part E, Supplemental Guidance for Dermal Risk Assessment). EPA/540/R/99/005
605 Office of Superfund Remediation and Technology Innovation; U.S. Environmental Protection
606 Agency, Washington, DC.
607 USEPA (2010) Residential tap water supporting table.
608 http://www.epa.gov/earth1r6/6pd/rcra_c/pd-n/screen.htm.
609 Varol M, Sen B (2012) Assessment of nutrient and heavy metal contamination in surface water
610 and sediments of the upper Tigris River, Turkey. Catena 92, 1-10.

611 https://doi.org/10.1016/j.catena.2011.11.011
612 Vega M, Pardo R, Barrado E, Deban L (1998) Assessment of seasonal and polluting effects on the
613 quality of river water by exploratory data analysis. Water Res 32, 3581-3592.
614 https://doi.org/10.1016/S0043-1354(98)00138-9
615 Vitola I, Vircavs V, Abramenko K, Lauva D, Veinbergs A (2012) Precipitation and air temperature
616 impact on seasonal variations of groundwater levels. Environ Clim Technol 10, 25-33.
617 https://doi.org/10.2478/v10145-012-0022-x
618 Wang J, Liu GJ, Liu HQ, Lam PKS (2017) Multivariate statistical evaluation of dissolved trace
619 elements and a water quality assessment in the middle reaches of Huaihe River, Anhui, China.
620 Sci Total Environ 583, 421-431. https://doi.org/10.1016/j.scitotenv.2017.01.088
621 Wang XL, Luo Y, Sun L, He CS, Zhang YQ, Liu SY (2016) Attribution of Runoff Decline in the
622 Amu Darya River in Central Asia during 1951-2007. J Hydrometeorol 17, 1543-1560.
623 https://doi.org/10.1175/JHM-D-15-0114.1
624 Whish-Wilson P (2002) The Aral Sea environmental health crisis. Rural Remote Health 1, 29-34.
625 https://www.researchgate.net/publication/237774223_The_Aral_Sea_environmental_health_cri
626 sis
627 WHO (2011) Guidelines for Drinking Water Quality, fourth ed. World Health Organization.
628 https://www.who.int/water_sanitation_health/publications/2011/dwq_guidelines/en/
629 Wu HW, Wu JL, Li J, Fu CS (2020) Spatial variations of hydrochemistry and stable isotopes in
630 mountainous river water from the Central Asian headwaters of the Tajikistan Pamirs. Catena
631 193, 104639. https://doi.org/10.1016/j.catena.2020.104639
632 Yang XW, Wang NL, Chen AA, He J, Hua T, Qie YF (2020) Changes in area and water volume of
633 the Aral Sea in the arid Central Asia over the period of 1960-2018 and their causes. Catena 191,
634 104566. https://doi.org/10.1016/j.catena.2020.104566
635 Zeng XX, Liu YG, You SH, Zeng GM, Tan XF, Hu XJ, Hu X, Huang L, Li F (2015) Spatial
636 distribution, health risk assessment and statistical source identification of the trace elements in
637 surface water from the Xiangjiang River, China. Environ Sci Pollut R 22, 9400-9412.
638 https://doi.org/10.1007/s11356-014-4064-4

Figures

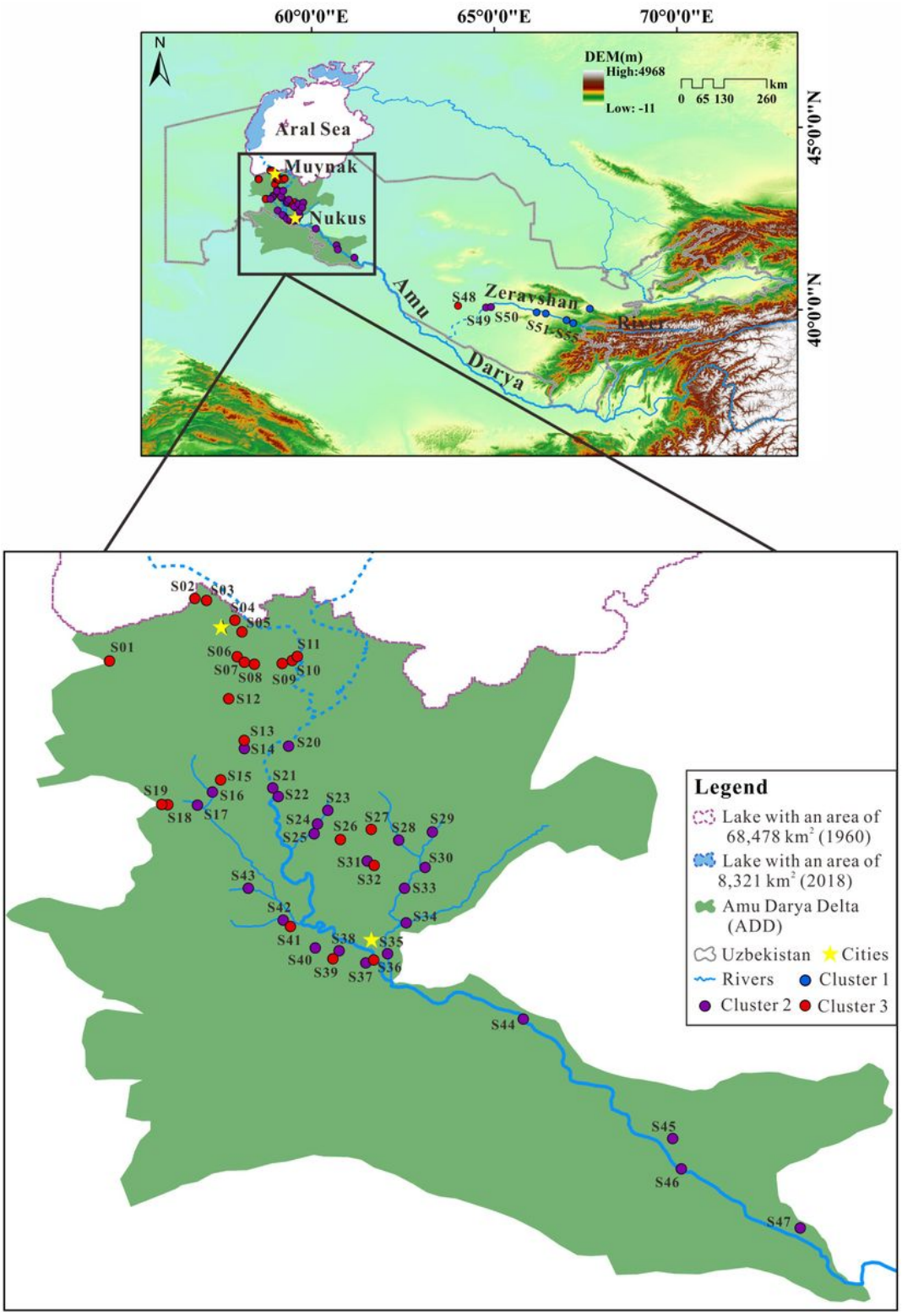

Figure 1

Geographical location of the study area and sampling sites Note: The designations employed and the presentation of the material on this map do not imply the expression of any opinion whatsoever on the part of Research Square concerning the legal status of any country, territory, city or area or of its

authorities, or concerning the delimitation of its frontiers or boundaries. This map has been provided by the authors.

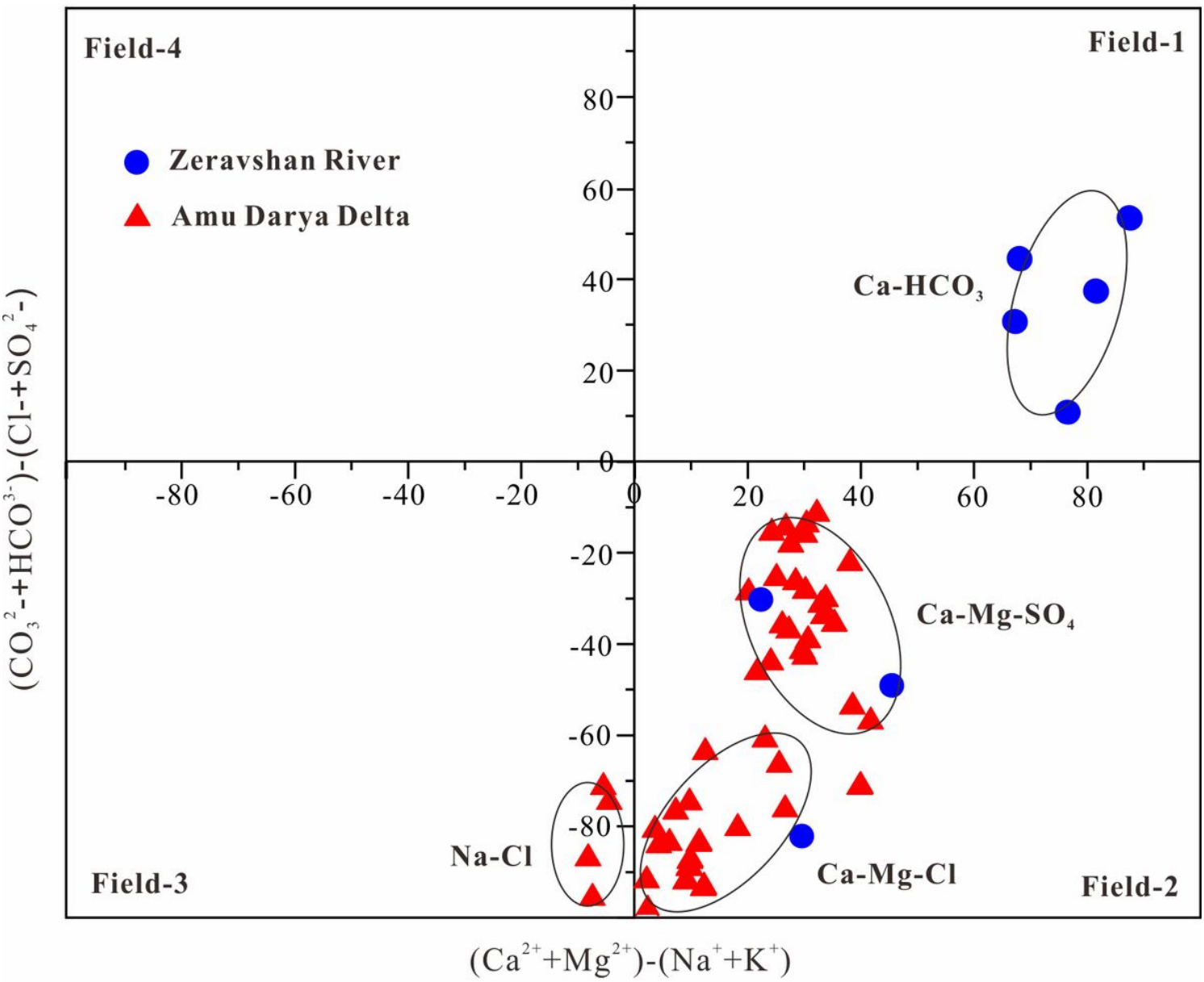

Figure 2

Chadha diagram demonstrating the hydrochemical classification of surface waters in the ADBU

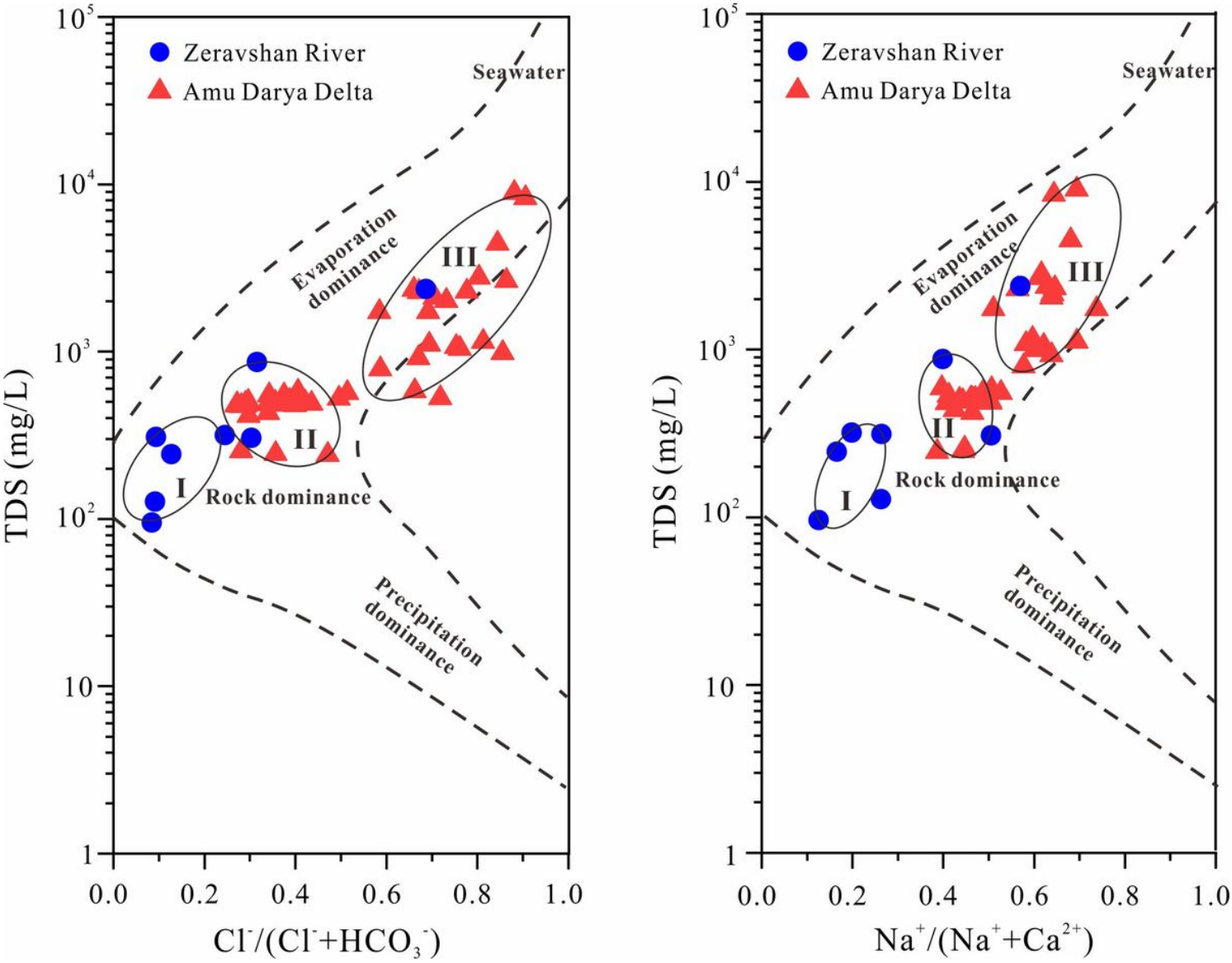

Figure 3

Gibbs diagram showing the main natural processes controlling hydrochemistry

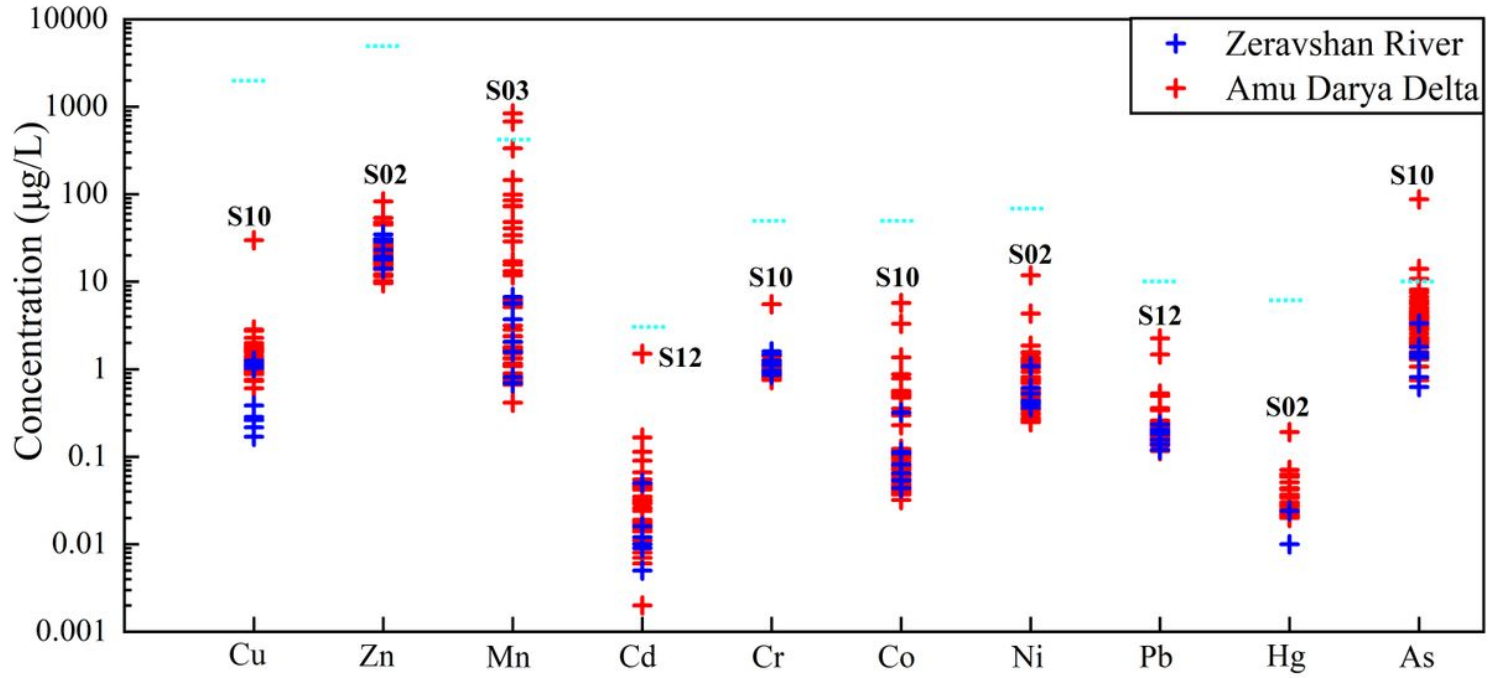

Figure 4

The toxic element concentrations of surface water in the ADBU. The blue dotted line indicates the drinking water standards of the WHO (2011)

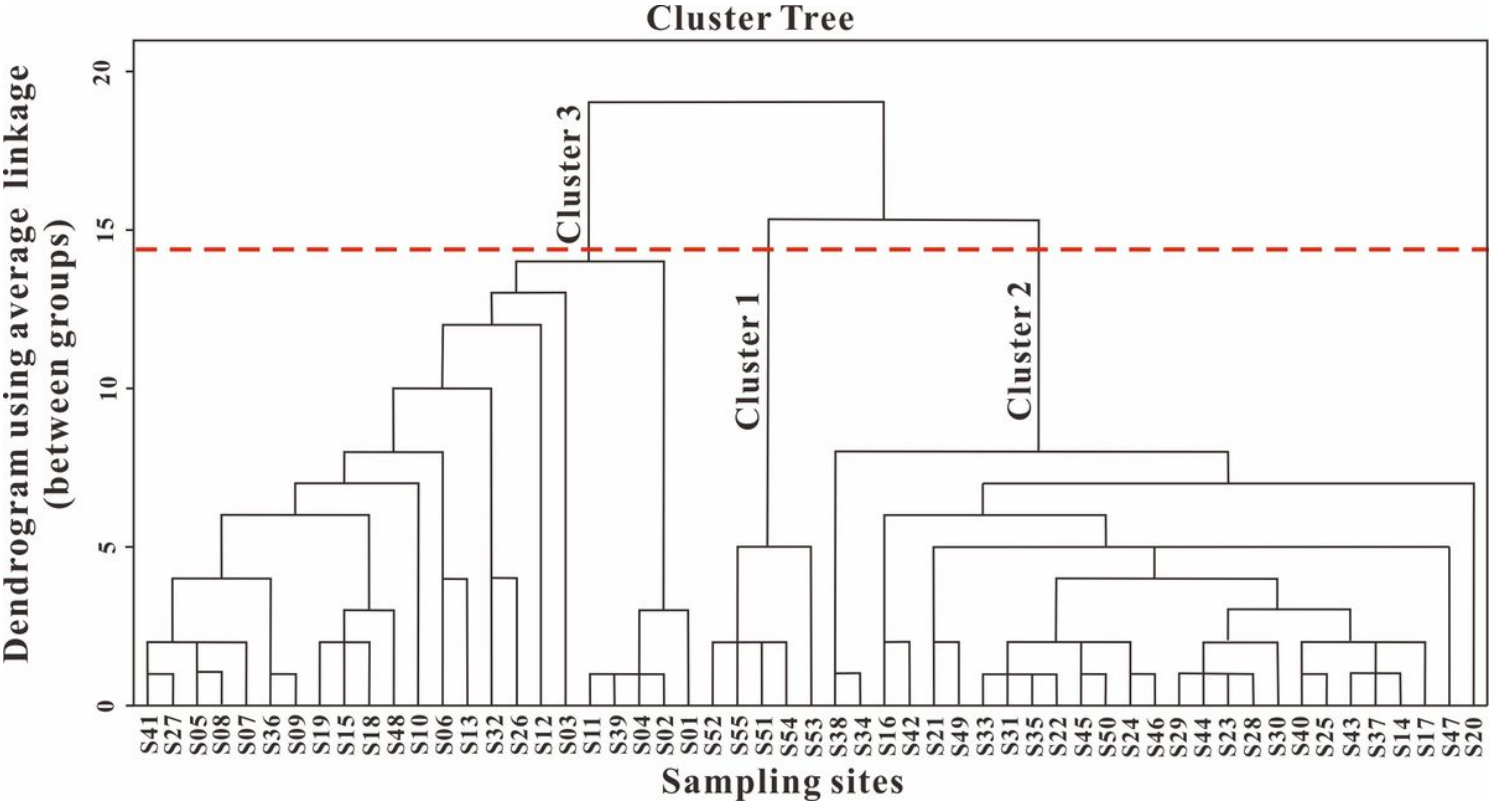

Figure 5

Dendrogram based on agglomerative hierarchical clustering for water samples in the ADBU.

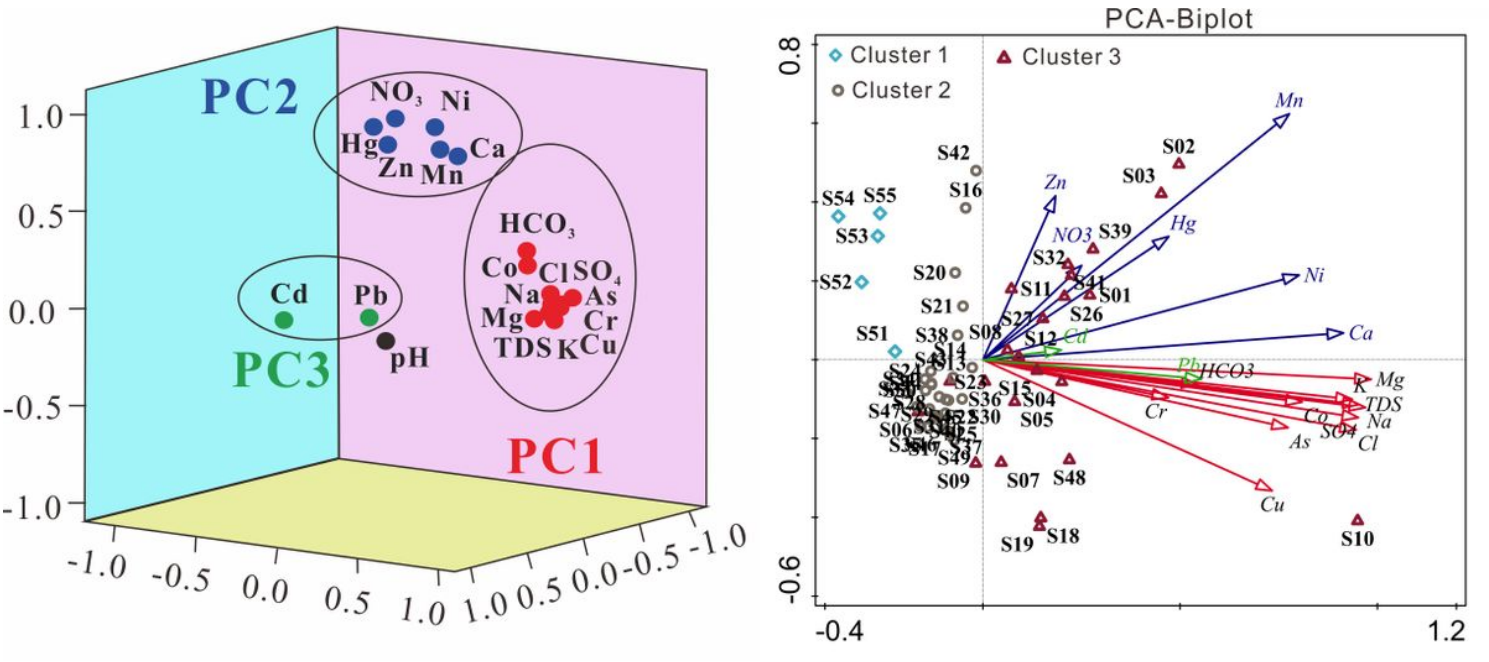

Figure 6

Principal component analysis (PCA) for toxic elements in surface waters in the ADBU. (a) Component plot in rotated space by using SPSS, and (b) loading plot in two dimensions by using Canoco.

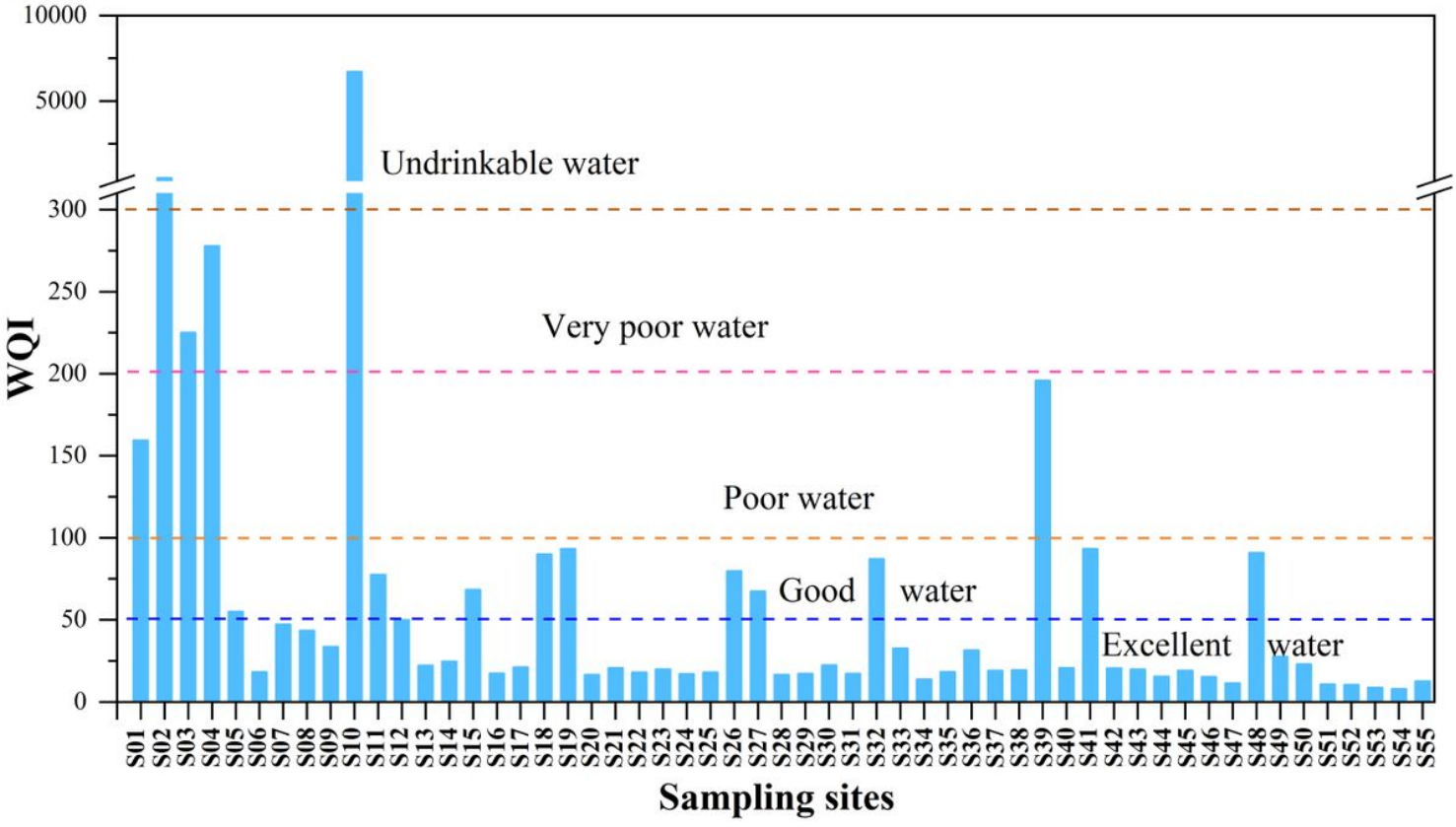

Figure 7

Water quality assessment by WQI values of surface water in the ADBU.

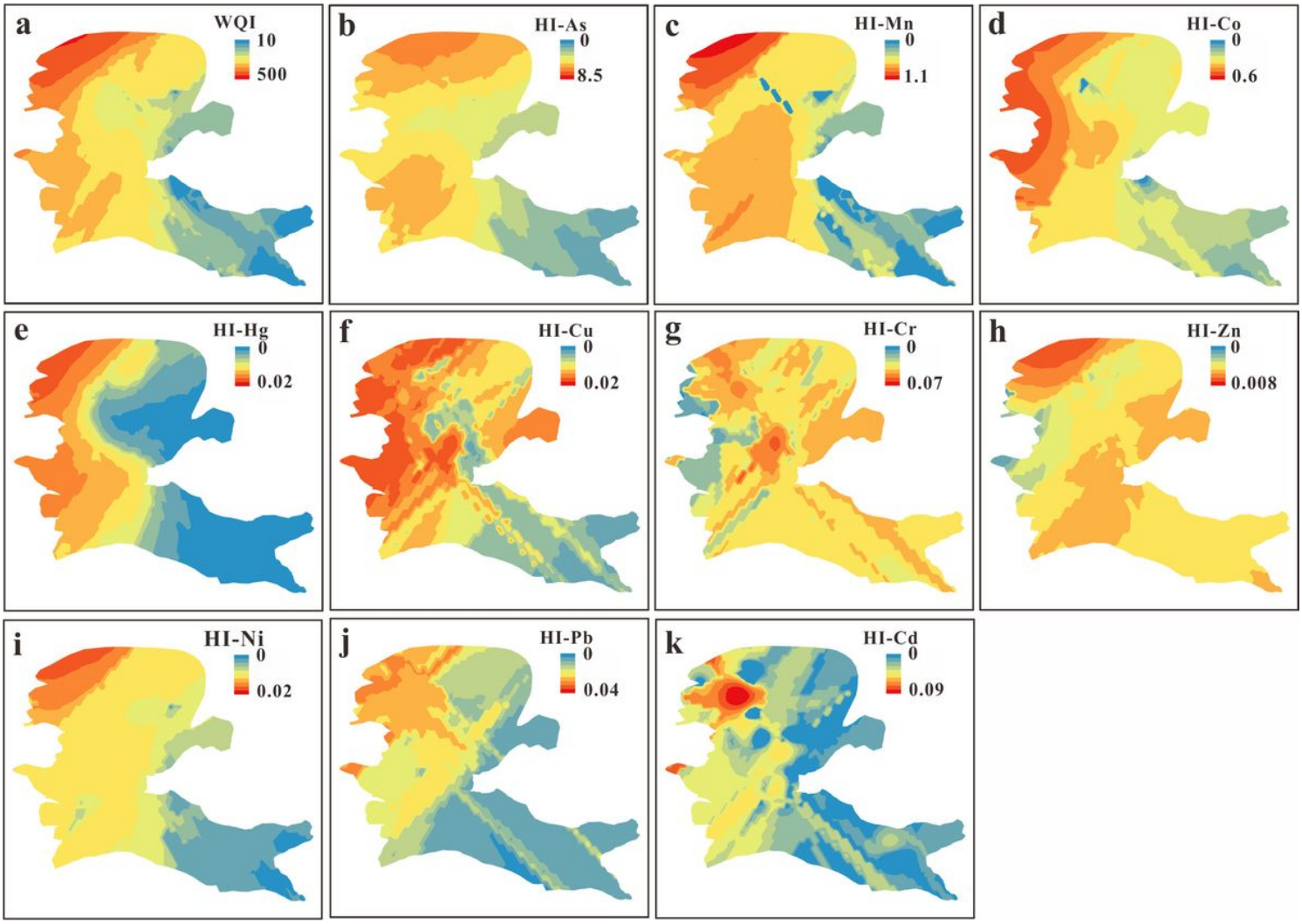

Figure 8

Spatial variations in the WQI (a) and HI (b-k) values for surface water in the ADD. Note: The designations employed and the presentation of the material on this map do not imply the expression of any opinion whatsoever on the part of Research Square concerning the legal status of any country, territory, city or area or of its authorities, or concerning the delimitation of its frontiers or boundaries. This map has been provided by the authors.

Supplementary Files

This is a list of supplementary files associated with this preprint. Click to download.

- Supplementarymaterial.doc